Massachusetts Institute of Technology
Center for Space Research
Cambridge, MA 02139
Room 37-558

To: ACIS Team
From: Takashi Isobe (ti@space.mit.edu)
Subject: Pix_dist Simulated Branching Ratio
Date: 10/25/96

This memo presents simulation results to provide references to lab data. Four subjects are presented:

1. Relation between a simulated data set and a lab data set.
2. Relation between a depletion depth and a branching ratio.
3. Relation between a split threshold and a branching ratio.
4. Secondary peaks and tail distributions.

1 Simulation: Pix_dist

X-ray CCD simulations are done by *Pix_dist*, a software developed by Andy Rasmussen (ACIS Memo #79). Given a fixed charge cloud evolution/drift model, *Pix_dist* estimates charge cloud distribution using Monte-Carlo method. The results are events list in *rv* format.

Although there are more than 30 different parameters to play with, we set following parameters for our simulations;

Option	Meaning	Value Set
-e	Energy in keV	see below
-n	Detected Events	100,000
-g	Linear Gain	4.0
-ne	Electron Readout Noise	2.5
-T	Temperature in K	153
-d	Depletion Depth in μm	70

Rv event files are created for C (0.277 keV), O (0.525 keV), F (0.677 keV), Al (1.489 keV), Si (1.740 keV), P (2.014 keV), Cl (2.622 keV), Ti (4.511 keV), V (4.952 keV), Fe55 (5.899 keV), Fe (6.404 keV), Co (6.930 keV), Ni (7.478 keV), Cu (8.048 keV), Zn (8.639 keV), and Ge (9.886 keV). The event files are further analyzed using $acisanal2$ with the event threshold 38 (ADU) and the split threshold 13 (ADU) or varied from 10 to 50 (ADU) for second experiment.

2 Comparison between a Simulated Data and a Lab Data

Table 1 shows a basic data for the simulated data set with the event threshold at 38 (ADU) and split threshold at 13 (ADU). Qdp files are created for grade 0 and grade 0234. A single Gaussian is fitted to a main peak. The counts in Table 1 is a peak count. The ratio g02346/total is the ratio of total counts between g02346 and g01234567.

Figure 1 plots the ratio g02346/total against the energy. We also plotted that from a lab data for w190c1 *beavis* experiment. Our simulation data does not follow the lab data well. The aluminum and copper are too low. This may be due to non-monochromatic nature of the sources, but we need to check further.

Energy (keV)	g0 Position (ADU)	Width (ADU)	Counts	g0234 Position (ADU)	Width (ADU)	Counts	g02346/Total
0.277	69.0212	3.64095	10741.0	69.0351	3.66150	10719.6	1.000
0.525	130.826	4.62955	7965.77	130.860	4.66709	8440.02	1.000
0.677	168.772	5.08296	7057.97	168.813	5.12178	7690.14	1.000
1.489	371.077	7.24075	3759.05	371.194	7.32224	5248.03	1.000
1.740	433.685	7.77023	3214.05	433.843	7.87027	4821.86	0.998
2.014	502.656	8.10541	3729.13	502.751	8.15907	4597.72	0.998
2.622	654.439	9.14943	3020.34	654.561	9.18972	4063.09	0.998
4.511	1126.24	11.7470	1767.51	1126.45	11.8468	3030.43	0.992
4.952	1236.33	12.2610	1604.20	1236.54	12.3366	2876.69	0.983
5.899	1472.92	13.3539	1292.59	1473.21	13.4436	2551.97	0.940
6.404	1598.98	13.9883	1180.18	1599.23	14.0670	2403.85	0.908
6.930	1730.36	14.5419	1064.34	1730.74	14.5498	2294.34	0.875
7.478	1867.18	14.9186	998.543	1867.61	15.0363	2188.58	0.841
8.048	2009.79	15.4512	920.891	2010.20	15.5499	2090.81	0.809
8.639	2157.38	16.0779	856.202	2157.79	16.1386	1995.36	0.780
9.886	2469.07	17.0694	749.826	2469.40	17.1336	1838.14	0.723

Table 1: Simulation Results: Basic Results

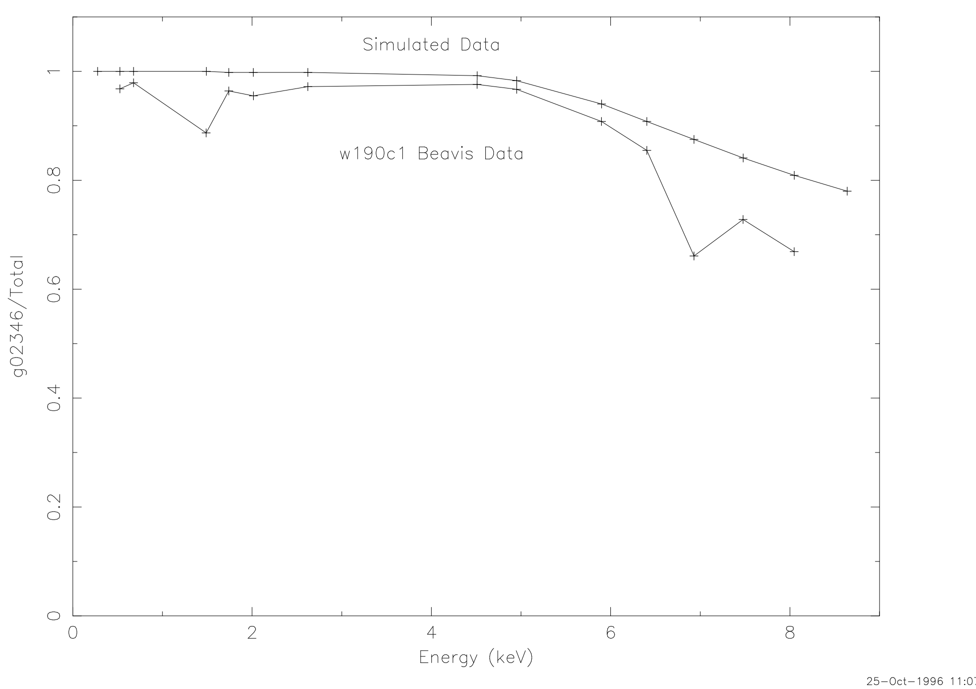

Figure 1: Comparison of Branching Ratios: w190c1 Beavis Data vs. Simulated Data

3 Depletion Depth and Branching Ratios

To see how the branching ratios depend on a depletion depth, we computed the branching ratio g0/g0234 for two points; Fe55 and Ge. The results are shown in Table 2 and 3. As the depletion depth increases, more g0 events occur. However, the line width does not change significantly.

Although g0/g0234 increases with the depletion depth increases, increasing the depletion depth alone does not correct the discrepancy seen in Figure 1. If we try to increase the ratio for Fe55 from 0.505 to 0.570 (lab data), the depletion depth needs to be more than 150 μm. This is not a realistic value for the depletion depth.

Depletion Depth (μm)	g0 Position (ADU)	Width (ADU)	g0234 Position (ADU)	Width (ADU)	g0/g0234
50	1472.64	13.4945	1472.93	13.5174	0.488
55	1472.95	13.4932	1473.17	13.5657	0.490
60	1472.68	13.3827	1473.06	13.4936	0.499
65	1472.82	13.4649	1473.11	13.5007	0.499
70	1472.92	13.3541	1473.21	13.4437	0.506
75	1472.85	13.3726	1473.14	13.4718	0.510

Table 2: Fe55 Depletion Depth Dependency

Depletion Depth (μm)	g0 Position (ADU)	Width (ADU)	g0234 Position (ADU)	Width (ADU)	g0/g0234
50	2468.69	17.1323	2469.30	17.2760	0.403
55	2468.87	17.1876	2469.39	17.3359	0.405
60	2468.91	17.2701	2469.31	17.2577	0.402
65	2468.98	17.1752	2469.35	17.1782	0.408
70	2469.07	17.0690	2469.40	17.1332	0.408
75	2468.84	16.9493	2469.42	17.1969	0.415

Table 3: Ge Depletion Depth Dependency

4 Split Threshold and Branching Ratio

A relation between a split threshold and a branching ratio are checked next. Table 4 shows branching ratios for each grade, g0234, and g02346 for selected elements. Figures 2 to 10 show the branching ratios for g0, g0234, and g02346. As expected, g0, g0234, and g02346 increase with the split threshold increases.

5 Secondary Peaks and Tail Distributions

Finally, we compared proportions of events in a primary peak, escape peak, fluorescence peak, and a tail. A single Gaussian model is fitted to each peak. The events in the tail is obtained by subtracting the all events in the peaks from the total counts of events.

The results are shown in Tables 5 and 6. The same information is plotted in Figure 11. About 3 to 4% of the events are detected in the secondary peaks and the tail portion of the distribution.

sp_th	g0	g1	g2	g3	g4	g5	g6	g7	g0234	g02346
O										
10	0.928	0.000	0.057	0.007	0.007	0.000	0.001	0.000	0.999	1.000
15	0.942	0.000	0.046	0.006	0.006	0.000	0.000	0.000	1.000	1.000
20	0.953	0.000	0.036	0.005	0.005	0.000	0.000	0.000	1.000	1.000
25	0.962	0.000	0.029	0.005	0.004	0.000	0.000	0.000	1.000	1.000
30	0.969	0.000	0.024	0.004	0.004	0.000	0.000	0.000	1.000	1.000
35	0.974	0.000	0.019	0.003	0.003	0.000	0.000	0.000	1.000	1.000
40	0.979	0.000	0.016	0.003	0.002	0.000	0.000	0.000	1.000	1.000
45	0.984	0.000	0.012	0.002	0.002	0.000	0.000	0.000	1.000	1.000
50	0.988	0.000	0.009	0.002	0.002	0.000	0.000	0.000	1.000	1.000
Si										
10	0.610	0.000	0.177	0.081	0.081	0.000	0.049	0.002	0.949	0.998
15	0.643	0.000	0.166	0.075	0.076	0.000	0.040	0.001	0.959	0.999
20	0.667	0.000	0.157	0.070	0.072	0.000	0.033	0.001	0.965	0.999
25	0.687	0.000	0.149	0.067	0.068	0.000	0.028	0.001	0.971	0.999
30	0.703	0.000	0.143	0.064	0.065	0.000	0.025	0.000	0.975	1.000
35	0.718	0.000	0.137	0.061	0.062	0.000	0.021	0.000	0.979	1.000
40	0.732	0.000	0.132	0.058	0.060	0.000	0.018	0.000	0.982	1.000
45	0.745	0.000	0.126	0.056	0.057	0.000	0.015	0.000	0.985	1.000
50	0.757	0.000	0.121	0.054	0.055	0.000	0.013	0.000	0.987	1.000
Fe55										
10	0.407	0.001	0.208	0.100	0.102	0.002	0.122	0.058	0.818	0.939
15	0.434	0.001	0.202	0.098	0.099	0.002	0.107	0.056	0.834	0.941
20	0.453	0.001	0.198	0.096	0.097	0.002	0.097	0.055	0.845	0.942
25	0.470	0.001	0.194	0.094	0.096	0.002	0.090	0.053	0.853	0.944
30	0.483	0.001	0.191	0.092	0.094	0.002	0.085	0.052	0.860	0.945
35	0.495	0.001	0.188	0.091	0.092	0.002	0.080	0.050	0.866	0.947
40	0.506	0.001	0.185	0.089	0.091	0.003	0.077	0.047	0.871	0.949
45	0.516	0.001	0.183	0.088	0.090	0.003	0.075	0.044	0.877	0.952
50	0.526	0.001	0.181	0.087	0.090	0.003	0.072	0.040	0.883	0.956
Ge										
10	0.228	0.000	0.171	0.085	0.085	0.002	0.151	0.277	0.569	0.721
15	0.248	0.000	0.170	0.085	0.084	0.002	0.137	0.274	0.587	0.724
20	0.262	0.000	0.169	0.084	0.084	0.002	0.126	0.272	0.599	0.726
25	0.273	0.000	0.168	0.084	0.083	0.002	0.118	0.271	0.609	0.727
30	0.284	0.000	0.167	0.084	0.082	0.002	0.112	0.269	0.617	0.729
35	0.293	0.001	0.166	0.083	0.082	0.002	0.108	0.265	0.624	0.732
40	0.301	0.002	0.166	0.083	0.082	0.005	0.108	0.254	0.632	0.739
45	0.312	0.004	0.166	0.083	0.082	0.009	0.108	0.236	0.644	0.752
50	0.331	0.006	0.167	0.083	0.082	0.009	0.105	0.217	0.663	0.768

Table 4: Split Threshold and Branching Ratio

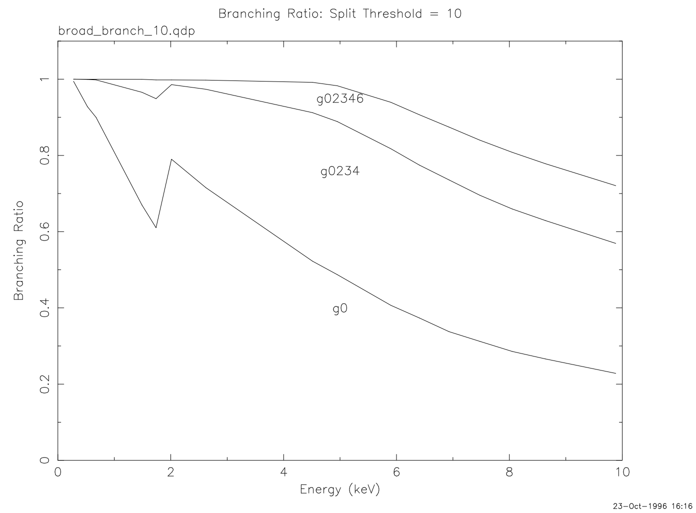

Figure 2: Branching Ratio for Split Threshold at 10 (ADU)

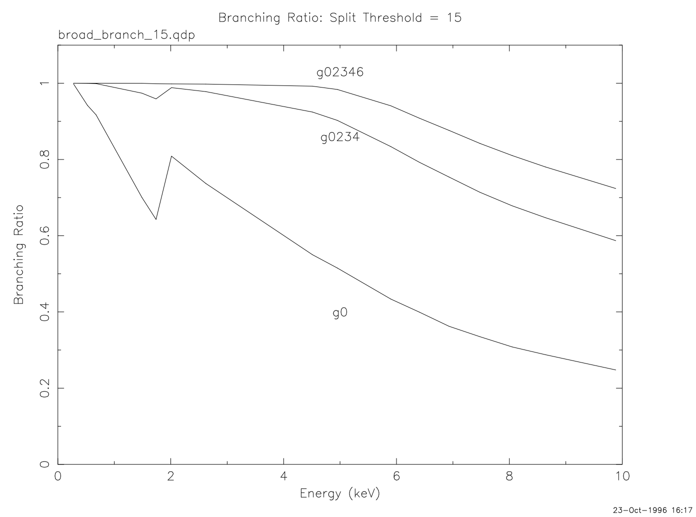

Figure 3: Branching Ratio for Split Threshold at 15 (ADU)

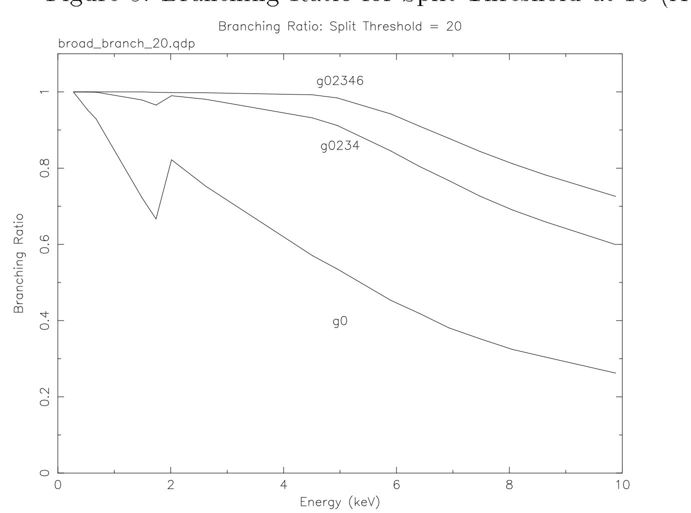

Figure 4: Branching Ratio for Split Threshold at 20 (ADU)

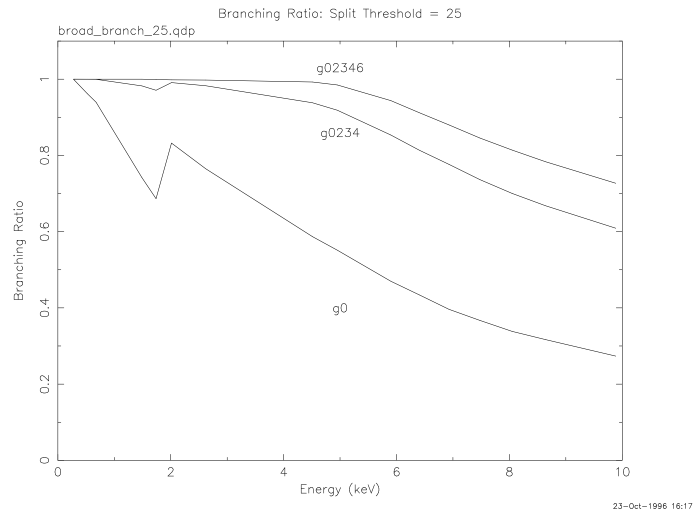

Figure 5: Branching Ratio for Split Threshold at 25 (ADU)

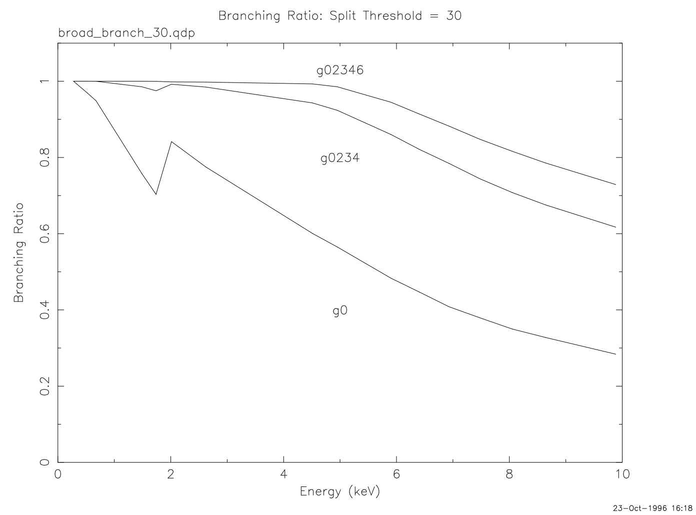

Figure 6: Branching Ratio for Split Threshold at 30 (ADU)

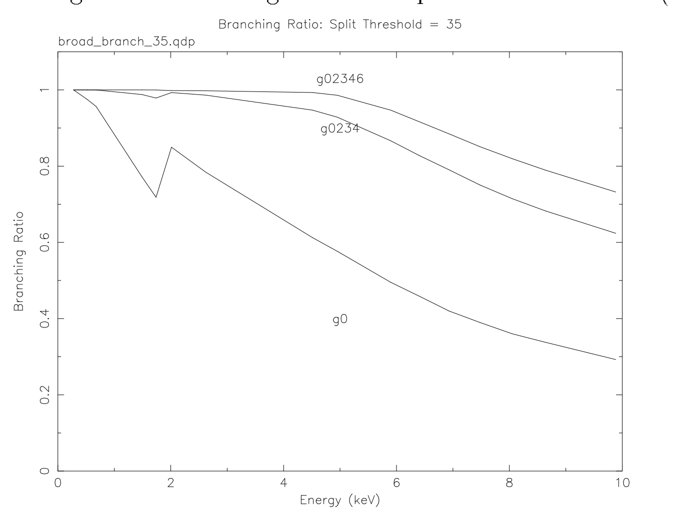

Figure 7: Branching Ratio for Split Threshold at 35 (ADU)

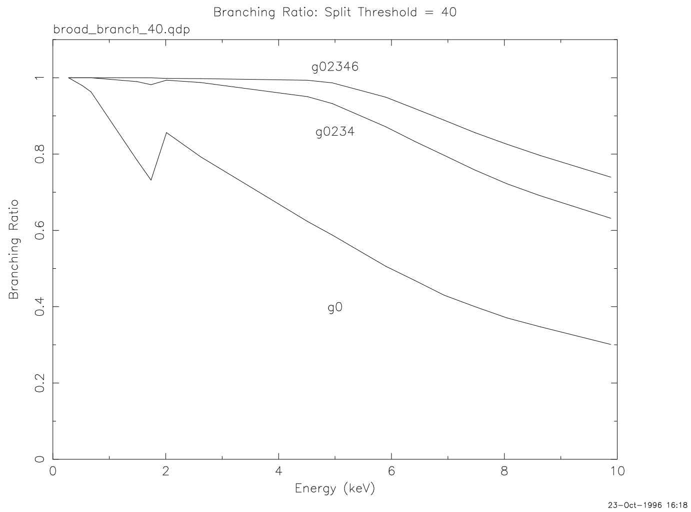

Figure 8: Branching Ratio for Split Threshold at 40 (ADU)

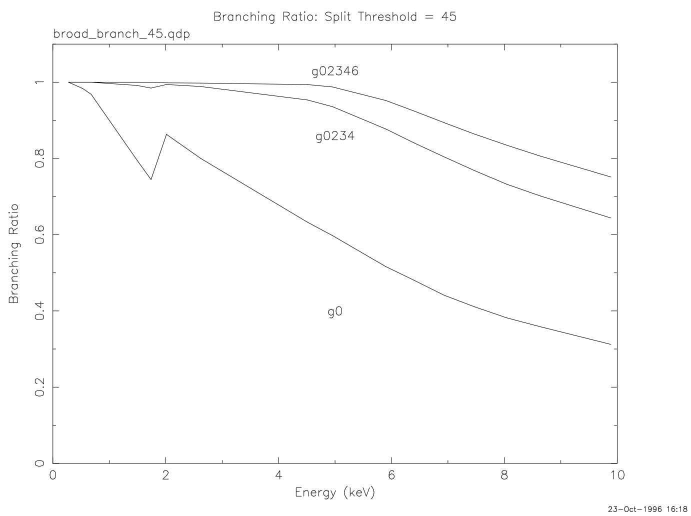

Figure 9: Branching Ratio for Split Threshold at 45 (ADU)

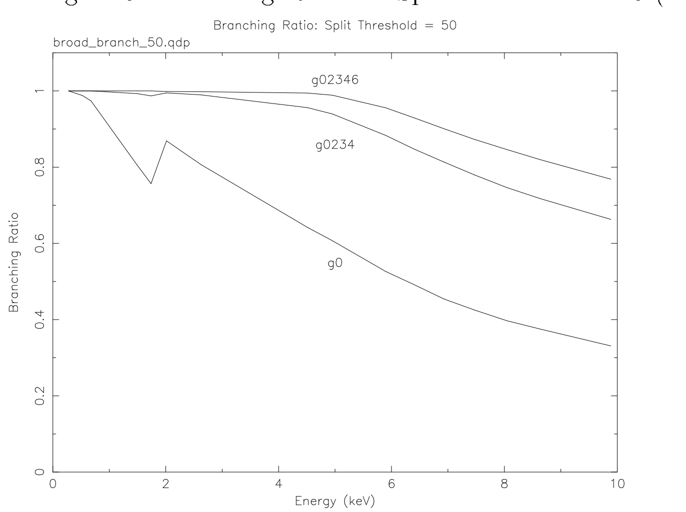

Figure 10: Branching Ratio for Split Threshold at 50 (ADU)

	Position (ADU)	Sigma (ADU)	Peak counts	Counts (Gaussian)		Counts (Total)
C (0.277 keV)						
primary:	69.0352	3.66151	10719.6	98385	(99.00%)	99374
tail:				989	(1.00%)	
O (0.525 keV)						
primary:	130.860	4.66711	8439.98	98737	(98.68%)	100057
tail:				1320	(1.32%)	
F (0.677 keV)						
primary:	168.813	5.12171	7690.25	98729	(98.39%)	100349
tail:				1620	(1.61%)	
Al (1.489 keV)						
primary:	371.194	7.32230	5247.99	96323	(98.78%)	97512
tail:				1189	(1.21%)	
Si (1.740 keV)						
primary:	433.842	7.87039	4821.82	95126	(98.96%)	96127
tail:				1001	(1.04%)	
P (2.014 keV)						
primary:	502.750	8.15911	4597.70	94031	(92.98%)	101130
escape:	68.5759	4.74079	141.083	1677	(1.66%)	
fluorescence:	435.031	14.3710	50.5146	1820	(1.80%)	
tail:				3602	(3.56%)	
Cl (2.622 keV)						
primary:	654.561	9.18979	4063.05	93594	(94.02%)	99552
escape:	219.726	6.56956	92.9726	1531	(1.54%)	
fluorescence:	433.403	15.5873	18.2930	715	(0.72%)	
tail:				3712	(3.73%)	
Ti (4.511 keV)						
primary:	1126.45	11.8470	3030.38	89990	(95.96%)	93775
escape:	692.238	10.1017	26.5548	672	(0.72%)	
fluorescence:	435.812	11.9897	5.13414	154	(0.16%)	
tail:				2959	(3.16%)	

Table 5: Secondary Peak Distribution C - Ti

	Position (ADU)	Sigma (ADU)	Peak counts	Counts (Gaussian)		Counts (Total)
V (4.952 keV)						
primary:	1236.54	12.3367	2876.66	88956	(96.28%)	92389
escape:	803.296	11.3480	19.7564	562	(0.61%)	
fluorescence:	435.642	13.3202	5.12338	171	(0.19%)	
tail:				2700	(2.92%)	
Fe55 (5.899 keV)						
primary:	1473.21	13.4435	2551.98	85996	(96.35%)	89253
escape:	1039.53	14.1055	13.7299	485	(0.54%)	
fluorescence:	431.943	16.9698	3.58848	153	(0.17%)	
tail:				2619	(2.93%)	
Fe (6.404 keV)						
primary:	1599.22	14.0673	2403.80	84762	(96.65%)	87699
escape:	1164.15	13.5739	10.3814	353	(0.40%)	
fluorescence:	431.678	15.3480	3.61246	139	(0.16%)	
tail:				2445	(2.79%)	
Co (6.930 keV)						
primary:	1730.74	14.5498	2294.35	83677	(96.56%)	86656
escape:	1298.79	18.9714	6.91177	329	(0.38%)	
fluorescence:	434.021	23.1022	2.56478	149	(0.17%)	
tail:				2501	(2.89%)	
Ni (7.478 keV)						
primary:	1867.61	15.0368	2188.52	82489	(96.50%)	85477
escape:	1433.54	14.7816	9.79103	363	(0.42%)	
fluorescence:	435.138	19.1750	3.52299	169	(0.20%)	
tail:				2456	(2.87%)	
Cu (8.048 keV)						
primary:	2010.20	15.5504	2090.73	81495	(96.56%)	84394
escape:	1574.26	22.0481	6.07928	336	(0.40%)	
fluorescence:	435.083	24.0338	2.40100	145	(0.17%)	
tail:				2418	(2.87%)	
Zn (8.639 keV)						
primary:	2157.79	16.1386	1995.36	80719	(96.35%)	83779
escape:	1723.20	18.1294	7.21554	328	(0.39%)	
fluorescence:	435.549	19.0470	2.91920	139	(0.17%)	
tail:				2593	(3.10%)	
Ge (9.886 keV)						
primary:	2469.40	17.1373	1837.79	78946	(96.14%)	82116
escape:	2035.03	22.9346	5.39062	310	(0.38%)	
fluorescence:	432.225	23.3047	2.03657	119	(0.14%)	
tail:				2741	(3.33%)	

Table 6: Secondary Peak Distribution V - Ge

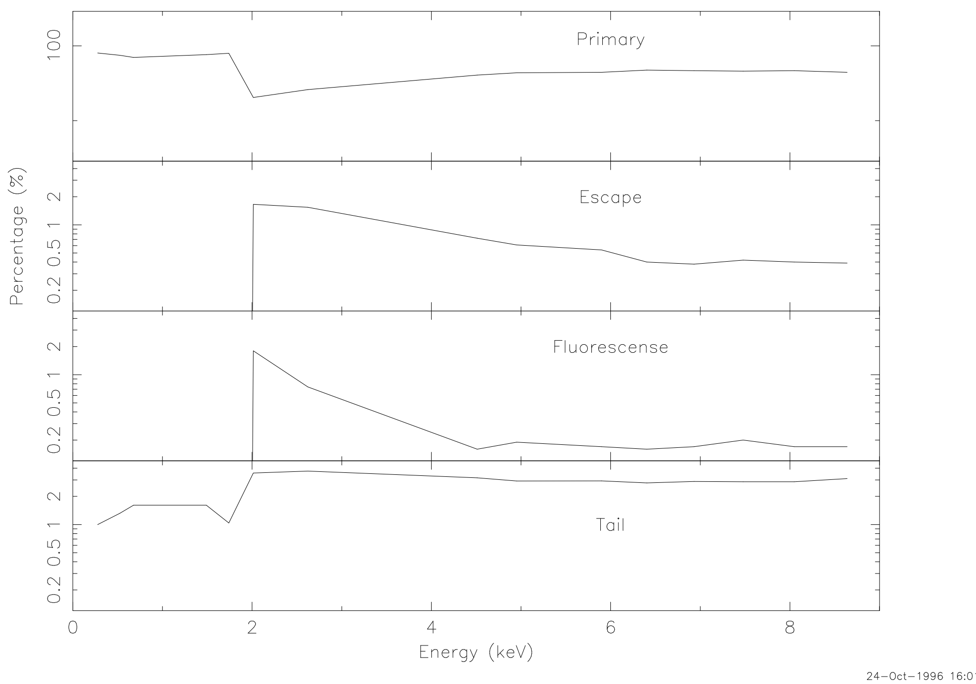

Figure 11: Percentage of Events Detected in Primary Peak, Escape Peak, Fluorescence Peak and Tail Counts